

Streaming current generation in two-phase flow conditions

Niklas Linde, D. Jougnot, André Revil, S. K. Matthäi, T. Arora, Didier Renard, Claude Doussan

► **To cite this version:**

Niklas Linde, D. Jougnot, André Revil, S. K. Matthäi, T. Arora, et al.. Streaming current generation in two-phase flow conditions. *Geophysical Research Letters*, American Geophysical Union, 2007, 34 (3), pp.L03306. 10.1029/2006GL028878 . insu-00404322

HAL Id: insu-00404322

<https://hal-insu.archives-ouvertes.fr/insu-00404322>

Submitted on 5 Mar 2021

HAL is a multi-disciplinary open access archive for the deposit and dissemination of scientific research documents, whether they are published or not. The documents may come from teaching and research institutions in France or abroad, or from public or private research centers.

L'archive ouverte pluridisciplinaire **HAL**, est destinée au dépôt et à la diffusion de documents scientifiques de niveau recherche, publiés ou non, émanant des établissements d'enseignement et de recherche français ou étrangers, des laboratoires publics ou privés.



Streaming current generation in two-phase flow conditions

N. Linde,^{1,2} D. Jougnot,^{1,3} A. Revil,^{1,4} S. K. Matthäi,⁵ T. Arora,^{1,6} D. Renard,⁷ and C. Doussan⁷

Received 24 November 2006; revised 3 January 2007; accepted 10 January 2007; published 13 February 2007.

[1] Self-potential (SP) signals that are generated under two-phase flow conditions could be used to study vadose zone dynamics and to monitor petroleum production. These streaming-potentials may also act as an error source in SP monitoring of vulcanological activity and in magnetotelluric studies. We propose a two-phase flow SP theory that predicts streaming currents as a function of the pore water velocity, the excess of charge in the pore water, and the porosity. The source currents that create the SP signals are given by the divergence of the streaming currents, and contributions are likely to be located at infiltration fronts, at the water table, or at geological boundaries. Our theory was implemented in a hydrogeological modeling code to calculate the SP distribution during primary drainage. Forward and inverse modeling of a well-calibrated 1D drainage experiment suggest that our theory can predict streaming potentials in the vadose zone. **Citation:** Linde, N., D. Jougnot, A. Revil, S. K. Matthäi, T. Arora, D. Renard, and C. Doussan (2007), Streaming current generation in two-phase flow conditions, *Geophys. Res. Lett.*, *34*, L03306, doi:10.1029/2006GL028878.

1. Introduction

[2] Recent results suggest that self-potential (SP) data could be efficiently used to study multi-phase flow processes in the vadose zone [e.g., *Thony et al.*, 1997; *Doussan et al.*, 2002] and in petroleum engineering [*Saunders et al.*, 2006]. *Thony et al.* [1997] found a strong linear relationship between the electrical field and the soil water flux at 40 cm depth at an agricultural test site following a rainfall event, and they suggested that SP data could be used to estimate water flux. *Doussan et al.* [2002] monitored SP signals in two lysimeters and found that there is no general relationship between SP and water flux, and that the slope of estimated relationships

changed over time. *Perrier and Morat* [2000] used data from a one-year electrode inter-comparison experiment to show that SP signals associated with evaporation might be of equal magnitude as reported earthquake precursors. In contrast to rainfall events that are monitored and known to produce SP signals, SP signals resulting from evaporation could potentially be interpreted as earthquake precursors. Understanding of SP signals is also necessary to improve the survey design and filtering of long-period magnetotelluric recordings [*Perrier and Morat*, 2000].

[3] Earlier attempts to model SP signals in the vadose zone have been based on the governing equations that apply to the saturated zone [*Sill*, 1983], but with the voltage coupling coefficient, C ($V Pa^{-1}$), assumed to be dependent on saturation [e.g., *Guichet et al.*, 2003; *Revil and Cerepi*, 2004; *Darnet and Marquis*, 2004; *Saunders et al.*, 2006]. *Guichet et al.* [2003] performed the first laboratory measurements of C as a function of saturation for an unconsolidated sand. They reported a threefold decrease of C at a saturation of 0.4 and a fivefold decrease in electrical conductivity as compared with saturated conditions. They proposed a model where C is linearly dependent on effective saturation. *Revil and Cerepi* [2004] measured C as a function of effective saturation for two dolomite samples and found a similar decrease of C . They developed a petrophysical model where the shape of the decrease of C includes the effect of surface conductivity. *Saunders et al.* [2006] simulated the SP response of a water-flood through a synthetic 3D reservoir model based on the functional relationship proposed by *Guichet et al.* [2003]. *Darnet and Marquis* [2004] performed synthetic 1D modeling of SP signals in the vadose zone and compared the results qualitatively with published field data. They assumed that C increases with decreasing saturation and they did not solve the Poisson equation that governs the SP distribution.

[4] Vadose zone dynamics are non-linear. Therefore, it is restrictive to assume that C has a linear dependence on effective saturation, or any other dependence that is assumed to be independent of soil or rock type. It is to be expected that this dependence is non-linear, that it varies among soil or rock types, and that it displays hysteresis. An alternative definition of C [*Revil and Leroy*, 2004] suggests that C is dependent on how the electrical conductivity [*Waxman and Smits*, 1968], the relative permeability [*van Genuchten*, 1980], and the excess of charge in the pore space vary as a function of saturation.

[5] Quantitative understanding of SP data collected in the vadose zone can only be obtained by modeling water flow in the vadose zone and by solving the Poisson equation that governs the SP distribution. Here, we propose a new model relating streaming currents in the vadose zone to the pore water velocity, the porosity, and the excess of charge of the pore fluid. Instead of introducing the coupling coefficient

¹Centre Européen de Recherches et d'Enseignement des Géosciences de l'Environnement, Département d'Hydrogéophysique et Milieux Poreux, Centre National de la Recherche Scientifique, Université Paul Cézanne, Aix-en-Provence, France.

²Now at Swiss Federal Institute of Technology, Institute of Geophysics, Zurich, Switzerland.

³Agence Nationale pour la Gestion des Déchets Radioactifs, Chatenay-Malabry, France.

⁴Groupement de Recherche Formations Géologiques Profondes, Agence Nationale pour la Gestion des Déchets Radioactifs, Centre National de la Recherche Scientifique, France.

⁵Department of Earth Science and Engineering, Imperial College, London, UK.

⁶Indo French Center for Groundwater Research, National Geophysical Research Institute, Hyderabad, India.

⁷Unité Climat, Sol et Environnement, Institut National de la Recherche Agronomique, Avignon, France.

and its dependence on saturation, the streaming currents dependency on saturation is modeled by well-known formula of how electrical conductivity and permeability vary with saturation. However, the coupling coefficient at saturation is needed to calculate the excess in charge of the pore fluid. Our model is tested against a column-scale experiment of primary drainage of a saturated and well-characterized sand during which we measured the resulting cumulative outflow of water, spatially variable capillary pressure at ten tensiometers, and the streaming potential on 17 non-polarizing Ag/AgCl electrodes.

2. Theory

[6] At the quasi-static limit, the total electrical current density, \mathbf{j} (A m^{-2}), is

$$\mathbf{j} = -\sigma \nabla \varphi + \mathbf{j}_s, \quad (1)$$

where σ is the electrical conductivity (assumed to be isotropic) (S m^{-1}), φ is the electrical potential (V), and \mathbf{j}_s is the streaming current density (A m^{-2}). The streaming current has two contributions in the vadose zone. The dominant contribution is related to ionic processes that occur in the vicinity of the surface of minerals in contact with water. The electrical double layer coating the surface of minerals implies the existence of a net excess of electrical charge in the pore water. The drag exerted on this—typically positive—excess of charge by the flow of pore water creates a polarisation of charge at the pore scale [e.g., *Revil et al.*, 1999]. The other contribution is caused by the negative charge at the air-water interface [*Yang et al.*, 2001] and it is negligible.

[7] The streaming current density is [*Revil and Leroy*, 2004]

$$\mathbf{j}_s = Q_v \mathbf{u}, \quad (2)$$

where \mathbf{u} and Q_v are the Darcy velocity (m s^{-1}) and the excess of charge in the water phase (C m^{-3}), balancing the surface charge at the solid-water interface. The relationship between Q_v and the excess of charge under saturated conditions, $Q_{v,\text{sat}}$, is given by

$$Q_v = \frac{Q_{v,\text{sat}}}{S_w}, \quad (3)$$

where S_w is the water saturation. From the interstitial velocity, \mathbf{u}/ϕ , where ϕ is the porosity, we derive an effective pore water velocity, \mathbf{v} , under partially saturated conditions

$$\mathbf{v} = \frac{\mathbf{u}}{S_w \phi}. \quad (4)$$

By inserting equations (3) and (4) into equation (2), \mathbf{j}_s becomes

$$\mathbf{j}_s = Q_{v,\text{sat}} \phi \mathbf{v}. \quad (5)$$

Consequently, the streaming current is linearly related to the effective pore water velocity and the excess of charge at saturated conditions. Equation (5) is at saturated conditions

equivalent to the classical formulation for streaming currents in the saturated zone [e.g., *Sill*, 1983]

$$\mathbf{j}_s = \sigma_{\text{sat}} C_{\text{sat}} \nabla P, \quad (6)$$

where σ_{sat} is the electrical conductivity of the water saturated porous material (S m^{-1}), C_{sat} is the voltage coupling coefficient at saturation (V Pa^{-1}) and P is the pressure (Pa). The relationship between C_{sat} and $Q_{v,\text{sat}}$ is given by [*Revil and Leroy*, 2004]

$$C_{\text{sat}} = -\frac{Q_{v,\text{sat}} k}{\mu_w \sigma_{\text{sat}}}, \quad (7)$$

where k is the permeability (m^2) (assumed to be isotropic) and μ_w is the dynamic water viscosity (Pa s).

[8] A similar derivation of the streaming current contribution associated with the air-water interface shows that this contribution is unlikely to be larger than 1% of \mathbf{j}_s at any S_w . There are three reasons for this: (1) the specific surface area of the solid-water interface for low S_w typically is three times larger than that of the air-water interface which decreases rapidly with S_w [e.g., *Brusseau et al.*, 2006]; (2) the surface charge density of the air-water interface is lower—by roughly 50%—than the surface charge density of mineral surfaces such as silica [*Yang et al.*, 2001; *Revil et al.*, 1999]; and (3) the resulting streaming current contribution is linearly dependent on S_w .

[9] The charge conservation in the quasi-static limit is

$$\nabla \cdot \mathbf{j} = 0. \quad (8)$$

Combining equations (1) and (8) yields a Poisson equation

$$\nabla \cdot \sigma \nabla \varphi = \nabla \cdot \mathbf{j}_s \quad (9)$$

governing the streaming potential distribution. Consequently, the sources that create the streaming potentials are located at boundaries where the divergence of equation (5) is non-zero. Such boundaries might in natural systems be the water table and capillary fringe, geological boundaries, or the confines of infiltration plumes caused by rainfall or irrigation.

[10] The electrical conductivity distribution needed to solve equation (9) can either be estimated from geophysical data, such as time-lapse electrical resistance tomography, or from simulated S_w using a hydrological model taking into account petrophysical constraints such as

$$\sigma = \sigma_{\text{sat}} \sigma_r \cong \sigma_{\text{sat}} S_w^n, \quad (10)$$

where n is Archie's second exponent. Other, more elaborate models for the relative electrical conductivity, σ_r , include the effects of surface conductivity.

[11] The best way to obtain \mathbf{v} , and thereby φ through the solution of equations (5) and (9) at all locations and times is through well-calibrated hydrological models. A suitable governing equation for the flow of slightly compressible water through non-deformable porous media at constant gas phase pressure is [*Richards*, 1931],

$$\phi \frac{\partial S_w}{\partial t} + \nabla \cdot \left[\frac{K(S_w)}{\rho_w g} \nabla (P_c(S_w)) - K(S_w) \mathbf{z} \right] = q_w, \quad (11)$$

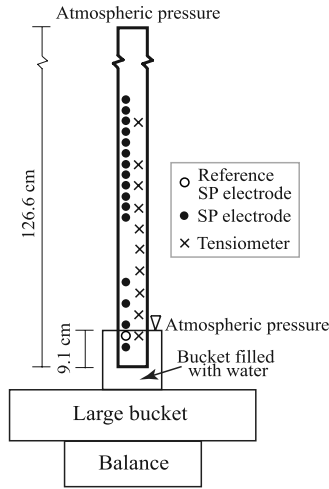


Figure 1. Experimental setup of the drainage experiment.

where t is time (s), K is the hydraulic conductivity (m s^{-1}), ρ_w is the water density (kg m^{-3}), g is the gravitational constant (m s^{-2}), P_c is the capillary pressure (Pa), \mathbf{z} is a vertically oriented unit vector (positive upward), and q_w is a source term (kg s^{-1}). The hydraulic conductivity is

$$K = k \frac{k_r(S_w) \rho_w g}{\mu_w}, \quad (12)$$

where the relative permeability of water $k_r(S_w)$ and $P_c(S_w)$ are often modeled using [van Genuchten, 1980]

$$k_r = \sqrt{S_e} \left[1 - \left(1 - S_e^{1/m} \right)^m \right]^2, \quad (13)$$

$$P_c = \frac{1}{\alpha} \left(S_e^{-1/m} - 1 \right)^{1-m}, \quad (14)$$

$$S_e = \frac{S_w - S_{wr}}{1 - S_{wr}}, \quad (15)$$

where S_e and S_{wr} are the effective and residual water saturations, respectively, and m and α (Pa^{-1}) are soil-specific parameters.

[12] Using equations (7), (10), and (13), we can derive the following expression for the voltage coupling coefficient as a function of saturation, $C(S_w)$, as

$$C(S_w) = \frac{C_{sat} k_r}{S_w \sigma_r}. \quad (16)$$

Consequently, the voltage coupling coefficient, C , varies non-linearly with saturation because both k_r (equation (13)) and σ_r (equation (10)) has a non-linear dependence on saturation. In addition, the voltage coupling coefficient is hysteretic as both k_r and σ_r are hysteretic. Perrier and Morat [2000] proposed a similar expression but without S_w . This means, that \mathbf{j}_s can either be calculated by equation (5) as we do in this work or by

$$\mathbf{j}_s = \sigma_{sat} \sigma_r C(S_w) \nabla P. \quad (17)$$

The two formulations are equivalent, but we favor equation (5) as only the effective pore velocity, v , is varying over time.

3. Laboratory Experiments

[13] A drainage experiment was performed in a poly vinyl chloride tube with an inner diameter of 35 mm and a length of 1350 mm. The sand used for the experiment was a fine grained quartz sand with a permeability of $7.9 \times 10^{-12} \text{ m}^2$ and a porosity in the range of 0.33–0.35. Tap water with an electrical conductivity of $\sigma_w = 0.051 \text{ S m}^{-1}$ was used. The electrical formation factor, F , of the sand is 4.26 ± 0.03 and surface conductivity is negligible. This allows $\sigma_{sat} = 0.012 \text{ S m}^{-1}$ to be estimated from $\sigma_{sat} = \sigma_w F^{-1}$. Using the protocol described by Suski *et al.* [2006], C_{sat} was estimated as $-2.9 \times 10^{-7} \text{ V Pa}^{-1}$, leading to an estimate of $Q_{v,sat}$ (see equation (7)) of 0.48 C m^{-3} for a μ_w of $1.14 \times 10^{-3} \text{ Pa s}$. Over a period of several hours, the sand was gradually saturated starting at the bottom of the tube to avoid trapping of air. Ten tensiometers and 17 non-polarizing Ag/AgCl SP electrodes were installed at different positions along the vertical tube (Figure 1). The tensiometric data were acquired with the WIND system of SDEC (www.sdec-france.com). The SP data were acquired with the ActiveTwo system of Biosemi (www.biosemi.com) at a sampling frequency of 512 Hz. The signals were filtered by calculating the median over periods of ten seconds.

[14] The first stage of the drainage experiment consisted of draining the saturated sand column, where the lower boundary condition consisted of a fixed head of 9.1 cm. The second stage of the experiment began after six hours when we removed the lower boundary (i.e., a bucket filled with water) to ensure free drainage. The resulting cumulative outflow (Figure 2), capillary pressures (Figure 3), and SP signals (Figure 4) are shown. The SP signals were shifted to ensure a zero-voltage at the end of each stage of the experiment where we assumed that water flow was insignificant.

[15] The hydraulic experiment was modeled with TOUGH2 [Pruess *et al.*, 1999], which is based on an integral finite difference method. We used a grid cell spacing of 0.5 cm. The capillary pressure and outflow data were fitted by inverting m of the relative permeability function (see equation (13)) and m and α of the capillary pressure function (see equation (14)) using iTOUGH2 [Finsterle, 1999], relying on its implementation of the downhill simplex algorithm. We estimated m of equation (13) to be 0.87, whereas α and m of equation (14) were

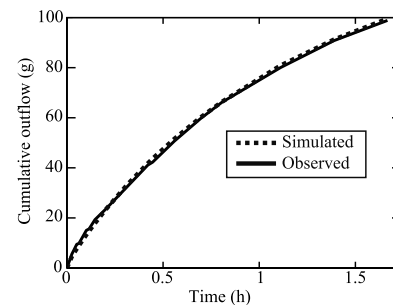


Figure 2. Simulated and observed cumulative outflow during the first stage of the drainage experiment.

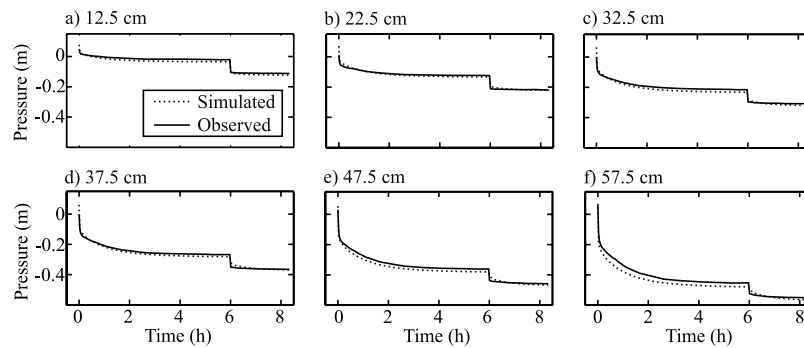


Figure 3. Simulated and observed capillary pressure data at selected locations. Distances (cm) are relative to the bottom of the column.

found to be $1.54 \times 10^{-4} \text{ Pa}^{-1}$ and 0.90, respectively. Figures 2 and 3 present a comparison between the simulated and observed cumulative outflow (RMS is 0.99 g) and capillary pressure data (RMS is 0.67 cm), respectively. The resulting calibrated hydrogeological model provides \mathbf{v} , which allows us to calculate \mathbf{j}_s from equation (5) using the measured values of ϕ and $Q_{v,sat}$ described above. The hydrogeological model also provides S_{vs} which allows an estimation of σ from equation (10), where we assumed that n is 1.6. Figure 4 provides a comparison between the predicted and measured SP data. The RMS data fit of the SP model is 0.125 mV. An equivalent solution can be obtained by calculating \mathbf{j}_s from equations (16) and (17).

[16] The right-hand side of equation (9) is completely dominated by the entries at the outflow location as $\nabla \cdot \mathbf{j}_s$ is insignificant within the column. The drainage experiment resulted in very small SP signals. Infiltration generally causes larger signals, (see Doussan *et al.* [2004], who monitored up to 40 mV difference in the electrical potential between 30 and 40 cm in a lysimeter filled with a sandy loamy soil).

4. Discussion and Conclusions

[17] Streaming potentials are caused by current sources that arise where there is a divergence of the pore water velocity and/or gradients of the porosity and the excess of charge in the pore space (see equations (5) and (9)). Self-

potential data collected at a specific location depend on current sources located throughout the investigated volume (see equation (9)) and large current sources at a distance may therefore hide the response of local variations in the vicinity of the measurement point. The magnitudes of the resulting streaming potentials are also affected by the electrical conductivity distribution of the medium (see equation (9)). Consequently, there can be no general linear relationship between unsaturated water flux and SP data as suggested by Thony *et al.* [1997] or between the local pressure gradient and SP gradient as suggested by Darnet and Marquis [2004].

[18] We argue that the theory presented in this paper is better suited to model SP signals in the vadose zone than prior adaptations of the saturated zone model [Sill, 1983] using a coupling coefficient that varies with saturation [Guichet *et al.*, 2003; Revil and Cerepi, 2004; Darnet and Marquis, 2004; Saunders *et al.*, 2006]. For completeness, we also derived an expression for how the coupling coefficient is expected to vary with saturation (see equation (16)). We postulate that the functional relationships that have been developed based on laboratory measurements [Guichet *et al.*, 2003; Revil and Cerepi, 2004] are not general, implying that they are of limited use for other soil and rock types, and flow conditions other than those investigated in the laboratory.

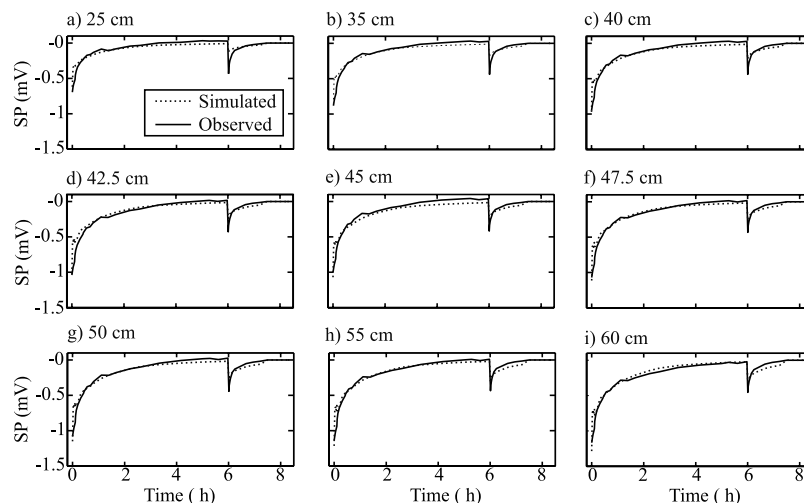


Figure 4. Simulated and observed SP data at selected locations. Distances (cm) are relative to the bottom of the column.

[19] The column experiment (Figure 1) was modeled and calibrated with outflow (Figure 2) and tensiometric data (Figure 3). The simulated pore water velocities and water saturations were used to calculate the SP distribution at different times. A comparison of the simulated and observed SP data (Figure 4) suggests that our new theory is capable of predicting SP signals in the vadose zone. The dominant SP source was situated where the water drains into a medium (water or air) where the excess of charge is zero. The streaming potential theory developed in this contribution applies equally well to the saturated zone.

[20] **Acknowledgments.** We thank the French “Direction de la Recherche” for a postdoctoral grant to N. Linde. The financial support of GDR-FORPRO (J. Lancelot) and ANDRA (S. Altmann and D. Coelho) is gratefully acknowledged. The Ph.D. thesis of D. Jougnot is supported by ANDRA. This is FORPRO contribution FORPRO 2006/19 A. We thank two anonymous reviewers for constructive reviews that helped to improve the clarity of the paper.

References

- Brusseau, M. L., S. Peng, G. Schnaar, and M. S. Costanza-Robinson (2006), Relationships among air-water interfacial area, capillary pressure, and water saturation for a sandy porous medium, *Water Resour. Res.*, *42*, W03501, doi:10.1029/2005WR004058.
- Darnet, M., and G. Marquis (2004), Modelling streaming potential (SP) signals induced by water movement in the vadose zone, *J. Hydrol.*, *285*, 114–124.
- Doussan, C., L. Jouniaux, and J.-L. Thony (2002), Variations of self-potential and unsaturated water flow with time in sandy loam and clay loam soils, *J. Hydrol.*, *267*, 173–185.
- Guichet, X., L. Jouniaux, and J. Pozzi (2003), Streaming potential of a sand column in partial saturation conditions, *J. Geophys. Res.*, *108*(B3), 2141, doi:10.1029/2001JB001517.
- Finsterle, S. (1999), iTOUGH2 user’s guide, *Rep. LBNL-40040*, Lawrence Berkeley Natl. Lab., Berkeley, Calif.
- Perrier, F., and P. Morat (2000), Characterization of electrical daily variations induced by capillary flow in the non-saturated zone, *Pure Appl. Geophys.*, *157*, 785–810.
- Pruess, K., C. Oldenburg, and G. Moridis (1999), TOUGH2 user’s guide, version 2.0, *Rep. LBNL-43134*, Lawrence Berkeley Natl. Lab., Berkeley, Calif.
- Revil, A., and A. Cerepi (2004), Streaming potentials in two-phase flow conditions, *Geophys. Res. Lett.*, *31*, L11605, doi:10.1029/2004GL020140.
- Revil, A., and P. Leroy (2004), Constitutive equations for ionic transport in porous shales, *J. Geophys. Res.*, *109*, B03208, doi:10.1029/2003JB002755.
- Revil, A., P. A. Pezard, and P. W. J. Glover (1999), Streaming potential in porous media: 1. Theory of the zeta potential, *J. Geophys. Res.*, *104*, 20,021–20,031.
- Richards, L. A. (1931), Capillary conduction of liquids through porous media, *Physics*, *1*, 318–333.
- Saunders, J. H., M. D. Jackson, and C. C. Pain (2006), A new numerical model of electrokinetic potential response during hydrocarbon recovery, *Geophys. Res. Lett.*, *33*, L15316, doi:10.1029/2006GL026835.
- Sill, W. R. (1983), Self-potential modeling from primary flows, *Geophysics*, *48*, 76–86.
- Suski, B., A. Revil, K. Titov, P. Konosavsky, M. Voltz, C. Dagès, and O. Huttel (2006), Monitoring of an infiltration experiment using the self-potential method, *Water Resour. Res.*, *42*, W08418, doi:10.1029/2005WR004840.
- Thony, J. L., P. Morat, G. Vachaud, and J. L. Le Mouél (1997), Field characterization of the relationship between electrical potential gradients and soil water flux, *C. R. Acad. Sci., Ser. IIA Sci. Terre Planetes*, *325*, 317–325.
- van Genuchten, M. T. (1980), A closed-form equation for predicting the hydraulic conductivity of unsaturated soils, *Soil Sci. Soc.*, *44*, 892–898.
- Waxman, M. H., and L. J. M. Smits (1968), Electrical conductivities in oil-bearing shaly sands, *Soc. Pet. Eng. J.*, *8*, 107–122.
- Yang, C., T. Dabros, D. Li, J. Czarnecki, and J. H. Masliyah (2001), Measurement of the zeta potential of gas bubbles in aqueous solutions by microelectrophoresis method, *J. Colloid Interface Sci.*, *243*, 128–135.

T. Arora, D. Jougnot, and A. Revil, CEREGE, Département d’Hydrogéophysique et Milieux Poreux, CNRS, Université Paul Cézanne, F-13545 Aix-en-Provence, France.

C. Doussan and D. Renard, Unité Climat, Sol et Environnement, INRA, F-84914, Avignon, France.

N. Linde, Institute of Geophysics, Swiss Federal Institute of Technology, CH-8093 Zurich, Switzerland. (linde@aug.ig.erdw.ethz.ch)

S. K. Matthäi, Department of Earth Science and Engineering, Imperial College, SW7 2AZ London, UK.